Defect Detection System for Smartphone Front Camera Based on Improved Template Matching Algorithm

Available online at www.sciencedirect.com

ScienceDirect

Procedia CIRP 103 (2021) 268–273

www.elsevier.com/locate/procedia

9th CIRP Global Web Conference – Sustainable, resilient, and agile manufacturing and service operations: Lessons from COVID-19

Defect Detection System for Smartphone Front Camera Based on Improved Template Matching Algorithm

Nengsheng Bao[a,b], Yuchen Fan[a,b], Alessandro Simeone[c]*, Tuyan Li[a,b], Zhaopeng Luo[a,b]

[a]*Intelligent Manufacturing Key Laboratory of Ministry of Education, Shantou University, Shantou, 515063, China*
[b]*Department of Mechanical Engineering, College of Engineering, Shantou University, Shantou 515063, China*
[c]*Department of Management and Production Engineering, Politecnico di Torino, 10129 Turin, Italy*

* Corresponding author. Tel.: +393517466999; *E-mail address:* alessandro.simeone@polito.it

Abstract

Automatic defect detection plays crucial role in resilient manufacturing in terms of product quality and cost effectiveness. With reference to the smartphone front cameras production process, the most recurrent defects can be classified into no hole, inner hole burr, outer circle damage, hole deformation, outer circle fracture and hole position offset. Due to the fast production lines and the defects micro size, Sampling-based methods has huge uncertainty and limitation, and Machine learning-based methods are characterised by low efficiency. To tackle these issues, this paper proposes a machine vision-based detection methods of smartphone front camera based on a multi-step template matching algorithm to reduce the computational effort. Specifically, in order to improve the algorithm efficiency, the images of the smartphone front cameras, acquired using industrial image acquisition devices are pre-processed by performing Hough circle and line transformations respectively, then locate the exact defect area as a region of interest (ROI). Finally, a multi-step template matching algorithm is used to detect and classify a number of common defects. Experimental results show an excellent suitability of the proposed system in detecting front camera surface defects. A benchmarking with other available technologies highlights how the proposed system yields an improvement in the detection speed by 46%, along with an improvement in the detection accuracy by 9%. The successful industrial implementation is discussed with reference to the integration into an automatic defect detection system in a smartphone front camera manufacturing context.

Peer-review under responsibility of the scientific committee of the 9th CIRP Global Web Conference – Sustainable, resilient, and agile manufacturing and service operations : Lessons from COVID-19 (CIRPe 2021)

Keywords: resilient manufacturing; process monitoring; image processing; template matching; defect detection

1. Introduction

Digital transformation of production processes and systems relies on Information and Communication Technologies (ICTs) to improve quality, productivity and sustainability [1, 2]. Such enabling technologies can effectively support the Zero-Defect Manufacturing (ZDM) paradigm, aimed at maximising the process reliability and the product quality by minimizing the defects on a production line [3]. At implementation level, the design and realisation of process monitoring systems can effectively reduce the overall product defect rate, strategic relevance in the long-term reliable operation of any automated controlled system [4]. Due to the increasing market share and constantly improved functionalities [5], an interesting manufacturing scope is represented by the smartphone front cameras production and assembly. A generic smartphone front camera internal structure is shown in Fig. 1. The overall assembly process is schematised in Fig. 2 and it can be summarised in the following steps: (1) manufacturing of lens and lens cone parts respectively; (2) lens and lens cone assembling and (3) light shield and spacer ring installation and gluing.

2212-8271 © 2021 The Authors. Published by Elsevier B.V.

Peer-review under responsibility of the scientific committee of the 9th CIRP Global Web Conference – Sustainable, resilient, and agile manufacturing and service operations : Lessons from COVID-19 (CIRPe 2021)
10.1016/j.procir.2021.10.043

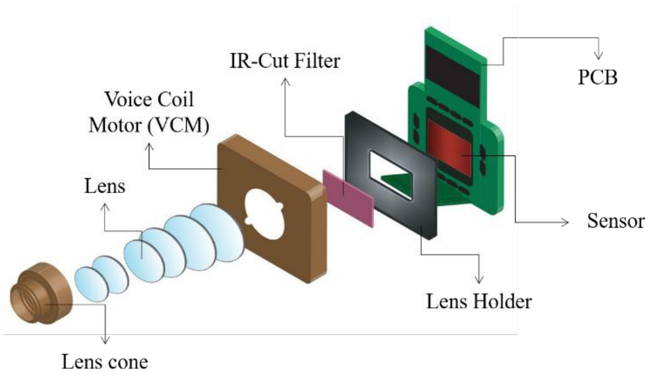

Fig. 1. Internal structure of a smartphone front camera

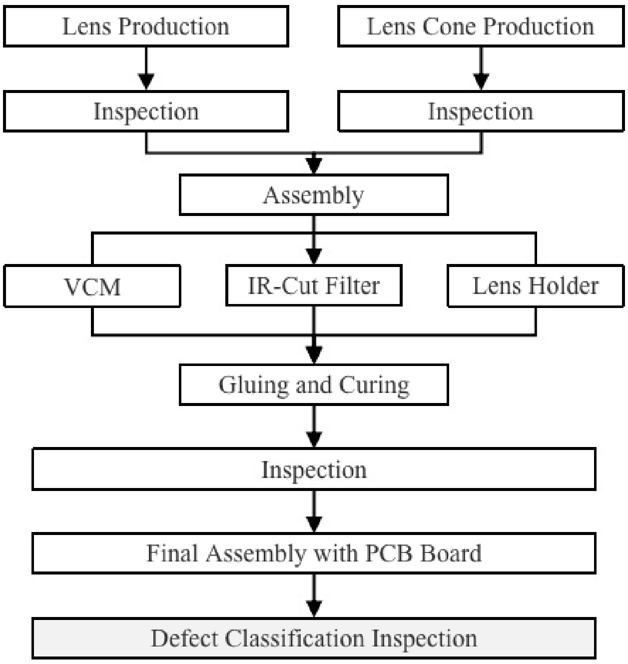

Fig. 2. Smartphone front camera production and assembly process

Following these steps, the camera is ready to be assembled to the PCB and image processor. During the assembly process, a critical step is represented by the performance defect classification inspection step (shaded box in Fig. 2). Due to its complexity, the assembly process is prone to a number of diverse uncertainties, including the technical factors, external environmental factors and human factors. Among them, the technical factors can be divided into parts aging, control system failure and nonlinear action and so on[6]. The external environmental factors of the project can be divided into unexpected climatic conditions and natural disasters. Human factors in engineering can be divided into engineering design concept defects, construction quality defects and operator malfeasance and other factors [6]. In this context, the prompt and accurate identification of production defects represents a critical aspect in the entire automated process inspection system, enabling the defects recognition and marking during the manufacturing process, allowing for a quick removal of defective parts from the assembly line and at the same time a statistical characterisation of defects for further statistical analysis. State-of-the-art defect detection methods for smartphone cameras can be classified in three types:

- Sampling-based methods: qualified staff selects a batch of products to manually carry out a surface inspection using a microscope to visually determine the presence of defects.
- Machine learning-based methods: such approaches perform pattern recognition tasks to classify defects using supervised learning paradigms such neural networks [7], support vector machines [8], and deep learning [9].
- Machine vision-based detection methods [10]: utilizing template matching algorithms [11], localisation algorithms, image processing-based features extraction [12] such as denoising, enhancement, edge detection etc. Machine vision technology has been widely used in industrial automation due to its flexible and efficient characteristics [13].

Sampling-based methods are characterised by high labour intensity and low detection efficiency, moreover detection results are easily affected by the skills and experience of the detection personnel [14], at the same time, when the defect size is less than 0.5 mm and there is no large optical deformation, the defect information cannot be detected by human eyes, representing an important limitation for large-scale industrial production. In addition, the quality of all front-facing cameras cannot be guaranteed due to the sampling-based inspection method, thus affecting the stability of product quality; machine learning methods generally have a higher accuracy in classification tasks, however they rely on the collection of a large number of samples to train the classifier [9], which is a complex process, and the real-time performance is poor, representing the most severe restriction in the application of such approaches. As regards the machine vision-based methods, although currently widely applied for matching purposes, they still present some drawbacks, such as excessive amount of computational effort, high time complexity and poor real-time performance [15, 16].

Taking into account the limitation of the current techniques, in order to carry out a reliable and efficient process monitoring, this paper proposes an optimised machine vision-based inspection system utilising an improved template matching algorithm. Such approach minimises the production chain interruptions caused by the non-conform front cameras, effectively reduces the error rate of the whole smartphone manufacturing process and improves the resilience of the automatic production system. Specifically, this paper adopts a strategy based on multi-step template matching, aimed at quickly identifying defects on the whole front camera surface during the production process, and qualitatively evaluates various defect types.

2. Materials and experimental setup

The machine vision-based monitoring system proposed in this paper includes an image acquisition unit and the visual detection system. The experimental rig realised for is shown in Fig. 3. The image acquisition unit consists in a charge-coupled device (CCD) digital industrial camera with a resolution of 2048 × 1536 pixels (3 Mpx). The optical lens has a focal length 8-75mm, to fulfil appropriate magnification and object distance requirements. As regards the light source, this consists of two elements, respectively a coaxial light ring and a backlight placed under the sample. Such experimental configuration allows to increase the contrast between the region of interest and other regions, to improve the image signal-to-noise ratio and to reduce the influence of material reflection, angle, and other factors such as external light etc. The computer is an Intel® Xeon® CPU E2-2620 v3@2.40GHz, Windows 10 operating system.

The visual detection system is composed of a camera module, communication module, image processing module and data storage module. The camera module is responsible for the image acquisition of the whole system. The communication module mainly exchanges data with the computer. The image processing module is responsible for analysing and processing the collected images. The data storage module is responsible for saving the results of the processing images.

3. Methodology

The experimental rig described above is used for the smartphone front camera defects detection.. Fig. 4 shows the image processing workflow for the defect identification and assessment.

The detailed procedure is reported in the remainder of this section. The proposed system focusses on the detection of six types of appearance defects of front camera reported as follows and illustrated in Fig. 5.

- No hole: there is no camera hole in the smartphone case.
- Lens stain: stains were detected on the lens inside the camera, and this detection will reduce the shooting capabilities of the smartphone front camera.
- Lens damage: this defect appears as a damage of the outer circle inner. It means the lens inside the camera is slightly damaged.
- Hole deformation: the whole camera slot has an unusual shape, this is most likely due to improper operation or device malfunction during the integration process.
- Lens cone fracture: this defect appears as a severe damage of the outer circle. It means the lens cone is totally broken and the ability of front camera to prevent dust is reduced.
- Hole position offset: The whole camera slot is out of position.

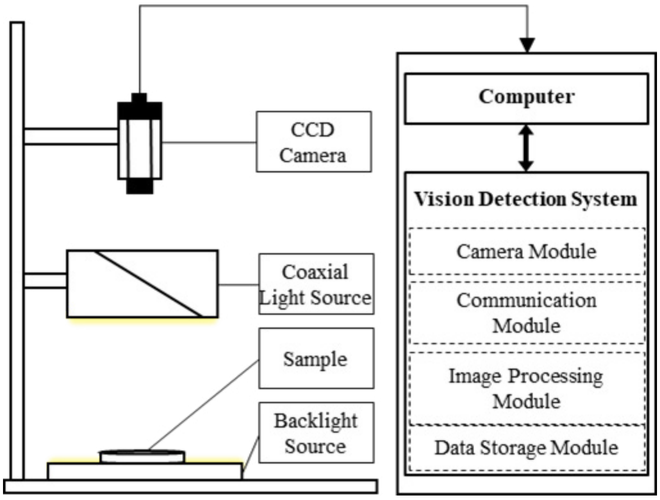

Fig. 3. Experimental setup

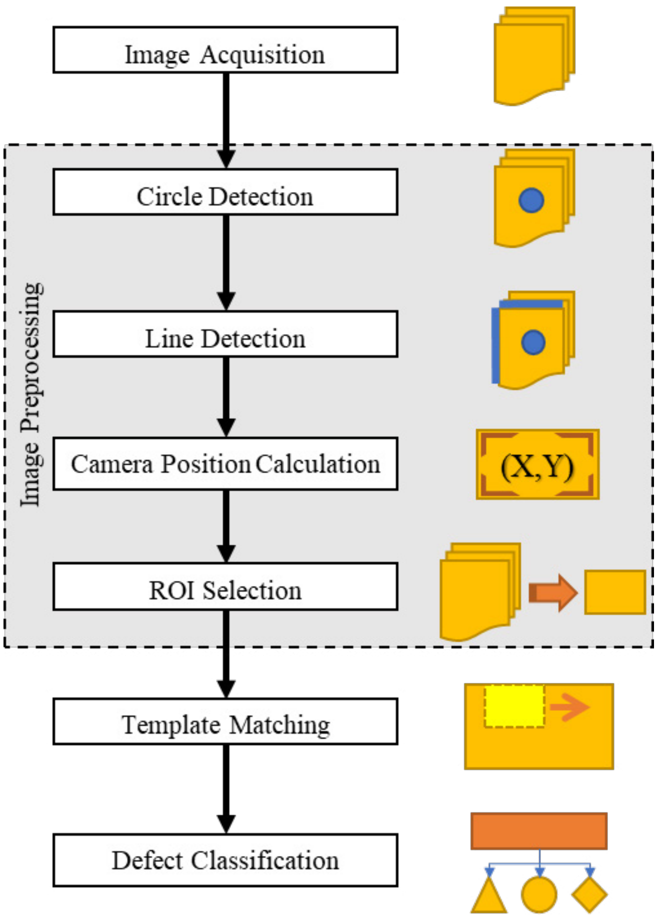

Fig. 4. Image processing flowchart

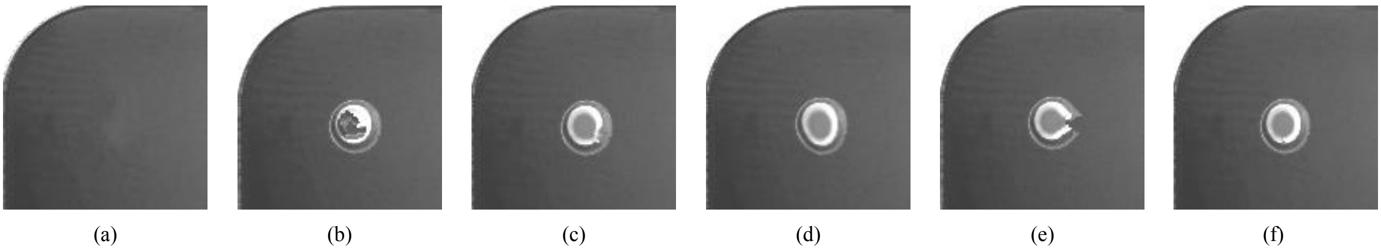

Fig. 5. Defects types: (a) No hole, (b) Lens stain, (c) Lens damage, (d) Hole deformation, (e) Lens cone fracture, (f) Hole position offset

3.1. Image pre-processing

Each smartphone camera raw image instance is subject to a pre-processing procedure aimed at identifying the region of interest containing the object to be detected and assessed, i.e. the smartphone front camera. Following the procedure reported in Fig. 4, the first step to identify the circular-shaped camera hole outline. In this respect, a Hough circle detection algorithm [17] is used to compute the coordinate (x, y) of the centre of the circle. Such approach has been adopted due to its reliability in terms of low sensitivity to noise, occlusions and varying illumination conditions [18]. The specific algorithm steps as follows:

Step 1. Input the digital image, set each edge points as (x_i, y_i), $i = 0, \ldots, N$ (N is the number of edge points);

Step 2. Set the double loop $x = (0, M)$, $y = (0, M)$ (where M is the resolution of the accumulation array) [17];

Step 3. Calculate the value of R by the formula R=$\sqrt{(x_i - x)^2 + (y_i - y)^2}$, then, add the values (x, y, R) to the accumulator for evaluation;

Step 4. Iterate over each edge point, finally the accumulator $[x, y, R]$ with the highest value is the detected circle.

Based on the same basic principle, a Hough Line Detection (HLD) algorithm [19] is used in this paper to detect the upper and left edges of the smartphone. Specifically, with reference to Fig. 6, the ordinate (Line 1) and the abscissa (Line 2) are firstly obtained via HLD, then the camera relative coordinates (Δ_x, Δ_y) can be retrieved, as graphically shown in Fig. 6. In order to enable a reliable defect classification with the minimum computation time, a Region of Interest (ROI) [19] is selected based on the information retrieved in the previous pre-processing steps. This paper utilises a rectangular 80×60 pixels ROI as shown in Fig. 6.

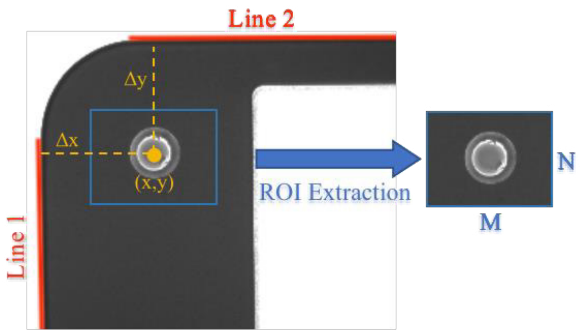

Fig. 6. Relative position of the camera and ROI extraction.

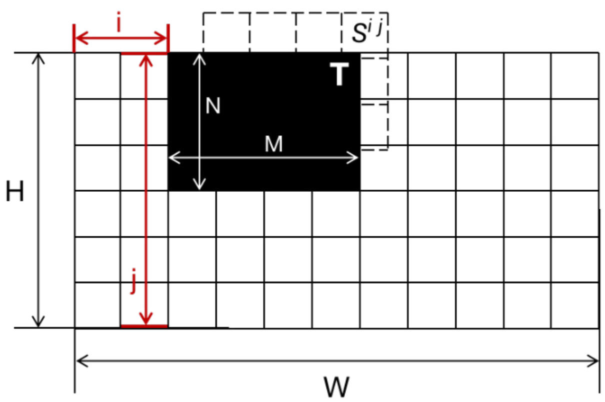

Fig. 7. Template matching algorithm mechanism

3.2. Template Matching

This section describes the two classification approaches considered in this paper, i.e. the standard and the improved template matching algorithms.

3.2.1. Standard Template Matching Algorithm

Template matching is an important part of digital image processing. Its essence is to measure the similarity between the input template and the sample. The best matching category of input template is the one with the largest similarity. The matching method is as follows: the input template is moved as a sliding window on the sample image from left to right and from top to bottom. After each pixel is moved, the "similarity" between image instance and template is calculated within the sliding window, and then compare the "similarity" results, the final maximum value is the best matching position of the input template in the sample. Such mechanism is shown in Fig. 7, where the similarity value between the input template and the sample is determined by the correlation coefficient R, computed as per Eq. (1) [20]:

$$R(i,j) = \sum_{m=1}^{M} \sum_{n=1}^{N} S^{ij}(m,n) * T(m,n) \qquad (1)$$

Where M and N are the width and the height of the template image respectively, $R(i,j)$ is the correlation coefficient, $S(m,n)$ is the sample to be detected, $S^{ij}(m,n)$ is the sub-graph of the sample to be detected, $T(m,n)$ is the input template, and (i,j) is the coordinate of the pixel in the upper left corner of the input template on the sample S. In correspondence of the largest value of R, the similarity value between the input template T and the sample S is the highest, and the best matching position is obtained.

3.2.2. Improved Template Matching Algorithm

The standard template matching (STM) algorithm is based on a sliding window matching procedure characterised by a step size of 1 px, therefore it needs to carry out one-by-one matches $(W - m + 1) \times (H - n + 1)$ times, resulting in a high computational effort and reduced efficiency.

To overcome this issue, this paper proposes an improved template matching (ITM) algorithm based on multi-step matching strategy, in which the template is overlapped on the image instance from left to right and from top to bottom, and the matching degree is calculated by the correlation coefficient R as per during the scanning process, so as to realise the extraction of defects. This strategy in each step of the matching process can equably cover the entire search sub-graph, and use these data to calculate correlation coefficient R can largely reduce error detection, so the algorithm not only can relieve the contradictions effectively, and also guarantee the template matching accuracy. The specific algorithm as follows:

Step 1. Upload the template T, superimpose it to S on the top-left corner, the pixel coordinate is (i, j).

Step 2. Compute the correlation coefficient R in the current position.

Step 3. Set the template T sliding window step size along x and y directions respectively as $S_x = m/4$, $S_y = n/4$. Such parameters have been experimentally determined.

Step 4. Slide the T window with S_x and S_y along x and y directions respectively and calculate the correlation coefficient R using the Eq. 1 in correspondence of the current window position.

Step 5. Repeat Step 4 Compute R at every iteration i, if $R_i > R_{max}$ go to Step 6, else if $R_i < R_{max}$ then return Step 3.

Step 6. Update $S_x = S_x/2$ and $S_y = S_y/2$, where 2 is an experimentally determined parameter selected to bring the matching value closer to the final position more accurately.

Step 7. Set an experimental termination threshold: if the current S_x and S_y >10E-6 then return to Step 4. Otherwise go to Step 8.

Step 8. Record the current position of the template (i, j) in correspondence of R_{max}.

Step 9. Repeat Steps 3-8 until covering the entire image S;

Step 10. Obtain R_{max} as the final maximum correlation coefficient, and the current recorded position as the template matching result.

4. Results and discussion

Both STM and ITM algorithms have been applied to an image dataset made of 60 image instances with the aim of classifying the six types of defects on front camera images described in Fig. 5. Each image instance has been processed and classified three times to improve the statistical reliability. This yielded to a total dataset made of 180 image instances. Two examples of image instances have been reported in Fig. 8. corresponding to lens cone fracture and hole position offset respectively. During the experimental tests, the image instances were collected from samples containing a large number of random defects, and then processed with both STM algorithm and the improved template matching algorithm respectively. The results are reported in the confusion matrices in Figs. 9-10 for the Standard and Improved template - matching algorithms respectively.

(e) (f)

Fig. 8. Example of test image instances: (e) Lens cone fracture, (f) Hole position offset.

Specifically, the confusion matrix in Fig. 9 shows that the STM algorithm correctly classifies 158 out of 180 image instances, yielding a total accuracy of 87.78%. As regards the ITM algorithm, the confusion matrix in Fig. 10 shows that the correctly classified image instances are 167 out of 180, yielding a higher total accuracy of 92.78%.

The benchmarking between the two algorithms under consideration includes the computation time. Such indicator has been computed as an average value over the total 180 image instances. The results reported in Table 1 show that the STM requires a computation time of 156 ms on average. As regards the ITM, Table 1 shows that this algorithm requires 92 ms on average. Table 1 indicates a very small worst performance of the ITM algorithm compared to the STM for the detection of hole deformation and hole position offset, although very small (2 ms).

The template matching method has the advantages of simplicity and directness, but it requires a fixed position of the object of interest, which is however not difficult to achieve with industrial equipment. Moreover, in a real industrial scenario, a batch of products is likely to include a large number of acceptable products and a small number of defective products.

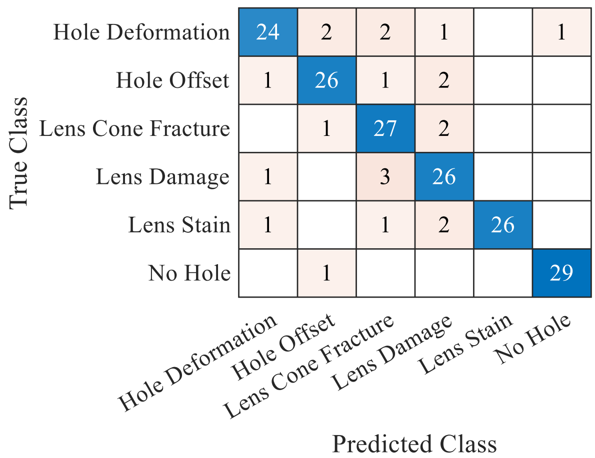

Fig. 9. Standard Matching Template Confusion Matrix

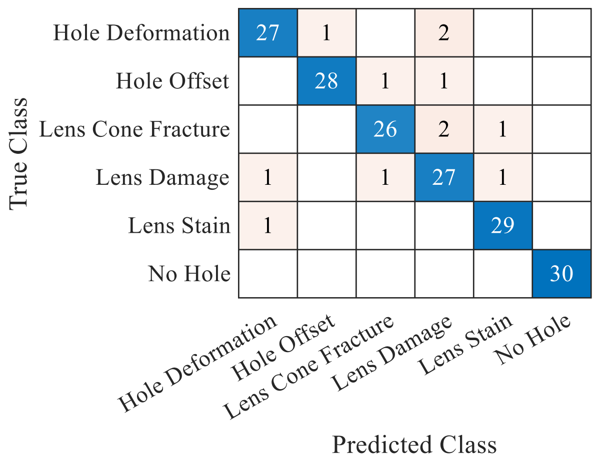

Fig. 10. Improved Matching Template Confusion Matrix

Table 1. Computation time comparison

Defect Type	Computation Time (ms)					
	STM			ITM		
	Min	Avg	Max	Min	Avg	Max
No hole	198	203	209	104	109	114
Inner hole burr	197	202	208	102	107	112
Outer circle damages	198	203	210	103	108	113
Outer circle fracture	199	204	211	102	107	112
Hole deformation	57	62	68	55	60	61
Hole position offset	57	62	68	55	60	61
Total average		**156**			**92**	

The acceptable products, having a higher matching rate due to their higher similarity to the template, will be classified in a shorter time compared to the defective products. This is due to the rapid updating of the step size resulting in a faster detection speed. In the experimental campaign it was recorded the ITM classification speed for acceptable products of 46 ms on average, which was much faster than the classification speed of 60 ms for acceptable products of the STM. Further improvement in terms of computation time can be achieved in an industrial environment with the use of more powerful computers, yielding to faster inspection capabilities compared to the laboratory scale. In terms of accuracy, there is still room for improvement. Higher definition cameras can be used to obtain clearer images, and uneven illumination correction method can also be carried out on the acquired images [21], so as to more accurately reflect the actual situation of the tested items and improve the accuracy of detection.

5. Conclusions

This paper proposed a machine vision-based inspection system aimed at detecting a number of defects during the assembly of smartphone front cameras using an improved template matching algorithm. In this context, an experimental campaign of image acquisition has been carried out on a tailored experimental rig. The acquired images were then subject to an image pre-processing procedure to identify the position of object of interest. i.e. the front camera unit. Subsequently, the template images were uploaded and the template matching algorithms were carried out on the image instances for the detection and the classification of six kinds of defects. Compared with the current manual inspection technique, the proposed method is more accurate, efficient and fast, with high degree of automation. These capabilities show a good potential suitability for industrial implementation both in terms of accuracy and computation time. In an actual industrial environment, each product could potentially have multiple defects. In this respect, future work will be focussed on the detection of overlapped defects, i.e. two or more defects simultaneously. Moreover, it is also necessary to address the trade-off between the matching accuracy and the computational speed, by improving the proposed algorithm in terms of a more efficient step size updating method.

Acknowledgements

This work was partially supported by the 2020 Li Ka Shing Foundation Cross-Disciplinary Research under Grant 2020LKSFG06D, the Research and application of defect image intelligent recognition system of Haimen Power Plant of Huaneng Power International Co. Ltd, China, (HM-19KA03005) and the research and modeling of economic operation efficiency of steam-driven induced draft fan under variable working conditions of Huaneng Shantou Haimen Power Generation Co. Ltd, China, (HZ-19ZC03-020).

References

[1] Gunasekaran A, , et al. Agile manufacturing: an evolutionary review of practices. Int J Prod Res 2019; 57(15–16):5154–74.

[2] Duo A, Segreto T, Caggiano A, et al. Drilling process monitoring: a framework for data gathering and feature extraction techniques. Procedia CIRP Elsevier 2021; 99:189–95.

[3] Stavropoulos P, Papacharalampopoulos A, Petridis D. A vision-based system for real-time defect detection: A rubber compound part case study. Procedia CIRP 2020[Online] Elsevier B.V. 2020.

[4] Severson K, Chaiwatanodom P, Braatz RD. Perspectives on process monitoring of industrial systems. Annu Rev Control Elsevier Ltd 2016; 42:190–200.

[5] Oh Y, Oh J. A critical incident approach to consumer response in the smartphone market: product, service and contents. Inf Syst E-bus Manag Springer Berlin Heidelberg 2017; 15(3):577–97.

[6] Zhengfeng L, Hangqing C, Qian W. Engineering ethics,. 2005[Online] 2005.

[7] Chang CY, Li CH, Chang YC, et al. Wafer defect inspection by neural analysis of region features. J Intell Manuf Springer 2011; 22(6):953–64.

[8] Chang C-F, Wu J-L, Chen K-J, et al. A hybrid defect detection method for compact camera lens. Adv Mech Eng 2017; 9(8):168781401772294.

[9] Caggiano A, Zhang J, Alfieri V, et al. Machine learning-based image processing for on-line defect recognition in additive manufacturing. CIRP Ann 2019; 68(1):451–54.

[10] Chauhan V, Surgenor B. Fault detection and classification in automated assembly machines using machine vision. Int J Adv Manuf Technol The International Journal of Advanced Manufacturing Technology 2017; 90(9–12):2491–512.

[11] Spratling MW. Explaining away results in accurate and tolerant template matching. Pattern Recognit Elsevier Ltd 2020; 104:107337.

[12] Zhao Z, Ren D, Zhao X, et al. Study on the Extraction Simulation of the Cylindrical Features. Math Probl Eng 2020; 2020:1–20.

[13] Malamas EN, Petrakis EGM, Zervakis M, et al. A survey on industrial vision systems, applications and tools. Image Vis Comput 2003; 21(2):171–88.

[14] Li H-S, Wang T, Yuan J-Y, et al. A sampling-based method for high-dimensional time-variant reliability analysis. Mech Syst Signal Process Elsevier Ltd 2019; 126:505–20.

[15] Mahmood A, Khan S. Correlation-coefficient-based fast template matching through partial Elimination. IEEE Trans Image Process 2012; 21(4):2099–108.

[16] Lin Y-H, Chen C-H. Template matching using the parametric template vector with translation, rotation and scale invariance. Pattern Recognit 2008; 41(7):2413–21.

[17] Zhou B, He Y. Fast Circle Detection Using Spatial Decomposition of Hough Transform. Int J Pattern Recognit Artif Intell 2017; 31(03):1755006.

[18] Canty MJ. Image Analysis, Classification, and Change Detection in Remote Sensing,. Image Analysis, Classification, and Change Detection in Remote Sensing 2019[Online] CRC Press 2019.

[19] Cai C, Chen L, Zhang X, et al. End-to-End Optimized ROI Image Compression. IEEE Trans Image Process IEEE 2020; 29(8):3442–57.

[20] Sonka M, Hlavac V, Boyle R. Image processing, Analysis, and Machine Vision-Cengage Learning,. 2014[Online] 2014.

[21] Dey N. Uneven illumination correction of digital images: A survey of the state-of-the-art. Optik (Stuttg) Elsevier 2019; 183(February):483–95.